Effect of Particle Size on the Performance of an N95 Filtering Facepiece Respirator and a Surgical Mask at Various Breathing Conditions

Xinjian He , Tiina Reponen , Roy T. McKay & Sergey A. Grinshpun

Effect of Particle Size on the Performance of an N95 Filtering Facepiece Respirator and a Surgical Mask at Various Breathing Conditions

Xinjian He, Tiina Reponen, Roy T. McKay, and Sergey A. Grinshpun

*Center for Health-Related Aerosol Studies, Department of Environmental Health,
University of Cincinnati, Cincinnati, Ohio, USA*

The effect of aerosol particle size on the performance of an N95 filtering facepiece respirator (FFR) and a surgical mask (SM) was evaluated under different breathing conditions, including breathing frequency and mean inspiratory flow (MIF) rate. The FFR and SM were sealed on a manikin headform and challenged with charge-equilibrated NaCl aerosol. Filter penetration (P_{filter}) was determined as the ratio of aerosol concentrations inside and outside the FFR/SM size-selectively (28 channels) within a range of 20 to 500 nm. In addition, the same models of the FFR and SM were donned, but not sealed, on an advanced manikin headform covered with skin-like material. Total inward leakage (TIL), which represents the total particle penetration, was measured under conditions identical to the filter penetration experiment. Testing was conducted at four mean MIFs (15, 30, 55, and 85 L/min) combined with five breathing frequencies (10, 15, 20, 25, and 30 breaths/min). The results show that SM produced much higher P_{filter} and TIL values, and thus provide little protection against aerosols in the size range tested. P_{filter} was significantly affected by particle size and breathing flow rate ($p < 0.05$) for the tested FFR and SM. Surprisingly, for both devices, P_{filter} as a function of the particle size exhibited more than one peak under all tested breathing conditions. The effect of breathing frequency on P_{filter} was generally less pronounced, especially for lower MIFs. For the FFR and SM, TIL increased with increasing particle size up to about 50 nm; for particles above 50 nm, the total penetration was not significantly affected by particle size and breathing frequency; however, the effect of MIF remained significant.

INTRODUCTION

N95 filtering facepiece respirators (FFRs) are commonly used to reduce occupational aerosol exposures. When certified by the National Institute for Occupational Safety and Health (NIOSH), N95 filters have a collection efficiency of at least 95% when tested against nonoil particles (e.g., NaCl) having a count median diameter (CMD) of 75 ± 20 nm with a geometric standard deviation (GSD) of <1.86 and a mass median aerodynamic diameter of ∼300 nm (NIOSH 1995). The NIOSH certification test utilizes the total particle concentration measurement based on the aerosol light scattering. Presently, the vast majority of FFRs are manufactured utilizing electrostatic fibers to enhance filter efficiency and, at the same time, reduce breathing resistance. Studies, which utilized a particle electrical mobility for the size-selective aerosol concentration measurement, have reported that the most penetrating particle size (MPPS) for N95 FFRs ranges from 30 to 100 nm (Martin and Moyer 2000; Grafe et al. 2001; Bałazy et al. 2006a,b; Eninger et al. 2008; Rengasamy et al. 2008; Cho et al. 2010a). Surgical masks (SMs) have a different intended purpose, and were originally designed to reduce bioaerosol dissemination from the wearer rather than to control wearer's exposure to ambient aerosols. Previous researches have demonstrated that the filter efficiency for SMs is much lower than that for N95 FFRs (Willeke et al. 1996; Bałazy et al. 2006a; Lee et al. 2008; Grinshpun et al. 2009).

The protection offered by an undamaged negative pressure air-purifying device (including N95 FFR and SM) depends on two principal factors: filter penetration (P_{filter}) and faceseal leakage ($P_{leakage}$) (Zhuang et al. 1998; Grinshpun et al. 2009; Cho et al. 2010b). The efficiency of respirator filter media has been assessed in several previous studies by measuring the aerosol concentration inside and outside of the FFR/SM while it was sealed to a manikin headform using constant or cyclic breathing flow (Bałazy et al. 2006b; Richardson et al. 2007; Cho et al. 2010b; Rengasamy and Eimer 2011; He et al. 2013d). To simulate faceseal leakage, artificially created slit-like or circular leaks have been commonly used in manikin-based respiratory protection research (Hinds and Bellin 1987; Myers et al. 1991;

Chen and Willeke 1992; Rengasamy and Eimer 2011). The limitation of most of the previous manikin-based faceseal leakage studies was that the headforms had rigid surfaces, which were unable to simulate the characteristics of the human skin. Ideally, it would be preferred to measure faceseal leakage while the respiratory protection device is donned on a human subject, not a manikin. However, respirator testing using humans has its own limitations, most importantly, the subjects cannot be exposed to hazardous aerosol challenges and it is impossible to maintain a constant leak size, shape, mean inspiratory flow (MIF), and breathing frequency (Wander et al. 2012). To partially address this limitation, an advanced manikin headform was recently developed with capabilities of mimicking the softness and thicknesses of the human skin (Hanson et al. 2006; Bergman et al. 2013).

Manikin-based respirator testing protocols using cyclic flow (as opposite to constant flow) produce data that more closely represent actual respirator use conditions. Unlike the constant flow utilized in many respiratory filtration studies, the cyclic flow is defined by two unique characteristics—mean inspiratory flow (L/min) and breathing frequency (breaths/min). It is acknowledged that the MIF affects the respirator filter efficiency. However, the effect of breathing frequency is still unknown. While evaluating respirators with cyclic flow, breathing frequency and flow rate should be tested as these two factors vary between populations (e.g., body size, age, health, etc.). Numerous studies have been conducted to evaluate effects of breathing flow rate and particle size on the performance of respiratory protection devices (Chen et al. 1990; Myers et al. 1991; Martin and Moyer 2000; Bałazy et al. 2006a,b; Eninger et al. 2008; Lee et al. 2008; Rengasamy et al. 2008; Cho et al. 2010a; He et al. 2013d). In contrast, the breathing frequency has been addressed only in a few investigations. One study (Wang et al. 2012) presented data only for two values, 32 and 50 breaths/min (which likely exceeds the breathing frequency for most worker populations that wear N95 FFRs and SMs) and a single MIF rate of 100 L/min (which is also higher than observed at nearly all workplace use conditions). Another investigation by our team evaluated the performance of an elastomeric half-mask respirator at different breathing frequencies, but not N95 FFRs and SMs (He et al. 2013a).

The present study is a follow-up to our recent effort in which the effect of breathing frequency on the performance of an N95 FFR and SM was examined particle-size-independently (He et al. 2013c). The experimental design used in the present study includes particle size as the main independent variable when testing the FFR/SM under various breathing conditions. The hypotheses of this study were: (1) the filter efficiency as well as the total inward leakage of FFRs and SMs are generally affected by the particle size, flow rate, and breathing frequency, and (2) for all tested particle sizes, breathing flow rates and frequencies, FFRs allow fewer particles to penetrate through than SMs (as determined by either filter efficiency or the total inward leakage).

MATERIALS AND METHODS

Tested N95 FFR and Surgical Mask

A widely used, commercially available N95 FFR having three layers with the middle being electrically charged to enhance the filter capture efficiency was chosen for this study. A conventional fluid resistant SM capable of providing at least 95% filter efficiency for 100 nm particles (according to the manufacturer) was also tested. To allow comparison with previous studies by our team, the selected FFR and SM was the same make and model as used previously (He et al. 2013c). To evaluate filter efficiency, the FFR/SM was fully sealed on a hard plastic manikin headform. The outcome of this experiment is not dependent on the properties of the manikin surface as long as a perfect sealing is achieved, which was confirmed using an air bubble detector. Additionally, the tested FFR/SM was donned on an advanced manikin headform without seal for the purpose of the total inward leakage (TIL = $P_{\text{filter}} + P_{\text{leakage}}$) testing. As the TIL depends on the headform surface properties (i.e., faceseal leakage), the advanced manikin with skin-like surface properties was utilized. After 20 consecutive tests, the FFR/SM was replaced with a brand new one to minimize the effect of the challenge aerosol loading on the filter media. Following each replacement, the particle concentrations inside and outside the FFR/SM were assessed to assure that the size of the leak was consistent with the one that existed before the change under the same experimental conditions. In addition, paired t-tests were performed to study the donning effect between the first 20 tests (before changing the FFR/SM) and the next 20 tests (after changing the FFR/SM), and the results showed that this effect was not significant ($p > 0.05$).

Experimental Design and Test Conditions

The experiments were carried out in a room-size (24.3 m³) respirator test chamber. Temperature and RH inside the chamber were kept at 17°C–22°C and 30%–60%, respectively. The experimental set-up was described in detail elsewhere (He et al. 2013c). In brief, NaCl particles (CMD = 125 nm, GSD = 1.68) generated with a particle generator (Model: 8026, TSI Inc., Shoreview, MN, USA) were first charge-equilibrated by passing through a [85]Kr electrical charge equilibrator (Model: 3054, TSI Inc., Shoreview, MN, USA) and then released into the test chamber. The headform with FFR/SM (either sealed in a filter penetration test, or donned in a total penetration test), was connected to a breathing recording and simulation system (BRSS, Koken Ltd., Tokyo, Japan). To keep particles from re-entering into the respirator cavity during exhalation cycles, a high-efficiency particulate air (HEPA) filter was placed between the headform and the BRSS. Prior to each experiment, the particle generator operated for at least 1 h to allow a uniform NaCl concentration inside the chamber, and continued operating during the testing to maintain a stable concentration level. It should be pointed out that, in contrast to FFRs, SMs are normally tested using nonneutralized particles although this is known to be less

than conservative approach given that electrically charged particles have greater capture efficiency (ASTM 1989, 2001; Oberg and Brosseau 2008; Rengasamy et al. 2009b). However, in order to compare the performances of the tested FFR and SM, in this study both devices were exposed to the charge-equilibrated challenge particles.

Cyclic breathing flows with MIF rates of 15, 30, 55, and 85 L/min and breathing frequencies of 10, 15, 20, 25, and 30 breaths/min were examined (total of 20 combinations). Each combination was tested in three replicates. Particle size-specific concentrations inside (C_{in_dp}) and outside (C_{out_dp}) of the FFR/SM were measured using a nanoparticle spectrometer (Nano-ID NPS500, Naneum Ltd., Kent, UK) operating in 28 channels within a range of $d_p = 20$–500 nm at a sampling flow rate of 0.2 L/min. The instrument measures particles based on their electrical mobility so that the particle number concentration determined for each channel represents the mean electro-mobility particle diameter corresponding to this channel. This outcome differs from the total particle concentration measured based on aerosol light scattering in the NIOSH respirator certification test. Each particle size-specific concentration (C_{in_dp} or C_{out_dp}) was determined based on a 6-min sampling.

For each mobility-based particle size, the filter penetration (P_{filter_dp}) was determined as the ratio of the corresponding size-specific number concentrations inside ($C_{\text{in}\_dp \text{ (Sealed)}}$) and outside ($C_{\text{out}\_dp \text{ (Sealed)}}$) of the FFR/SM sealed to the plastic headform:

$$P_{\text{filter}\_d_p} = \frac{C_{\text{in}\_d_p \text{ (Sealed)}}}{C_{\text{out}\_d_p \text{ (Sealed)}}} \times 100\%. \qquad [1]$$

The same experimental protocol and test conditions were used with FFR/SM donned (not sealed) on the advanced manikin headform for TIL measurements. Accordingly, the size-specific TIL values were determined as follows:

$$\text{TIL}_{d_p} = \frac{C_{\text{in}\_d_p \text{ (Donned)}}}{C_{\text{out}\_d_p \text{ (Donned)}}} \times 100\%. \qquad [2]$$

Data Analysis

Statistical data analysis was conducted using SAS version 9.3 (SAS Institute Inc., Cary, NC, USA). Three-way analysis of variance (ANOVA) was performed to study the effects of particle size, breathing frequency, and flow rate on the P_{filter} and TIL separately. A t-test was used to examine the differences in P_{filter} and TIL between the N95 FFR and the SM. For all data analyses, $p < 0.05$ represented significance.

RESULTS AND DISCUSSION

N95 Filtering Facepiece Respirator

N95 FFR Filter Penetration (P_{filter_dp})

Figure 1 presents the size-specific P_{filter_dp} values for the tested N95 FFR. It is seen that filter penetration increased with

increasing MIF ($p < 0.05$), which is consistent with the results of many previous N95 FFR studies (Bałazy et al. 2006b; Eninger et al. 2008; Rengasamy et al. 2008; Cho et al. 2010a; ; He et al. 2013a).

Particle size had a significant effect on the P_{filter_dp} ($p < 0.05$). Interestingly, all the filter penetration curves show two peaks for all MIFs and breathing frequencies, indicating two possible MPPS for the tested N95 FFR. The first MPPS occurred at 30–40 nm, which was expected for N95 FFRs composed of electrically charged fibers. Several studies have reported that the MPPS for an N95 FFR "electret" filter is <100 nm while a "mechanical" filter has an MPPS of approximately 300 nm (Martin and Moyer 2000; Bałazy et al. 2006a,b; Huang et al. 2007; Eninger et al. 2008; Rengasamy et al. 2009a). The second MPPS identified at ~300 nm (Figure 1) was not reported in any of the above quoted studies. One possible reason is that the quoted investigations (except the study conducted by Rengasamy et al. [2009a]) utilized a constant flow design, whereas the present effort represents a cyclic flow condition. It is possible that under the cyclic flow some particles are trapped inside the respirator cavity. This phenomenon "artificially" increases the particle count inside the FFR, thus affecting the filter penetration calculated by Equation (1). The effect is expected to be particularly pronounced at low C_{out_dp}. The tested aerosol is characterized by a rapidly decreasing concentration in the particle size range of 200 to 400 nm—the area where the second peak was identified (Figure 1). The other possible reason of the observed departure of $P_{\text{filter}} = f(d_p)$ from the conventional single-mode function could be associated with a three-layer filter structure of the tested N95 FFR of which only the middle layer was electrostatically charged. The combination of electrostatic (the middle layer) and mechanical (the two outer layers) characteristics may produce a compound penetration function involving particle diffusion, polarization force, interception, and impaction, which is capable of generating two peaks. Alternatively, the second peak may be attributed to limitations associated with the mobility-based particle measurement in the 100–500-nm size range, specifically with biases in corona charging and uncertainties in defining charge as a function of the particle size for particles that differ by morphology and other characteristics (Dhaniyala et al. 2011). The above could affect the particle concentration values in this size range and consequently lead to an aberration of the penetration curve at $d_p > 100$ nm, especially for lower concentrations measured inside the respirator. Future studies are needed to determine if the observed second peak can, at least partially, be linked to the instrumental error. We envision that such a study would utilize mobility classified challenge aerosol particles (as an alternative to the polydisperse NaCl aerosol used in the present study).

The effect of breathing frequency on filter penetration was complex and heavily dependent on the particle size and the MIF. This effect was most clearly seen for particles around the MPPS (Figure 1). For example, at the first MPPS (30–40 nm) the lower breathing frequencies (10, 15, and 20 breaths/min) produced
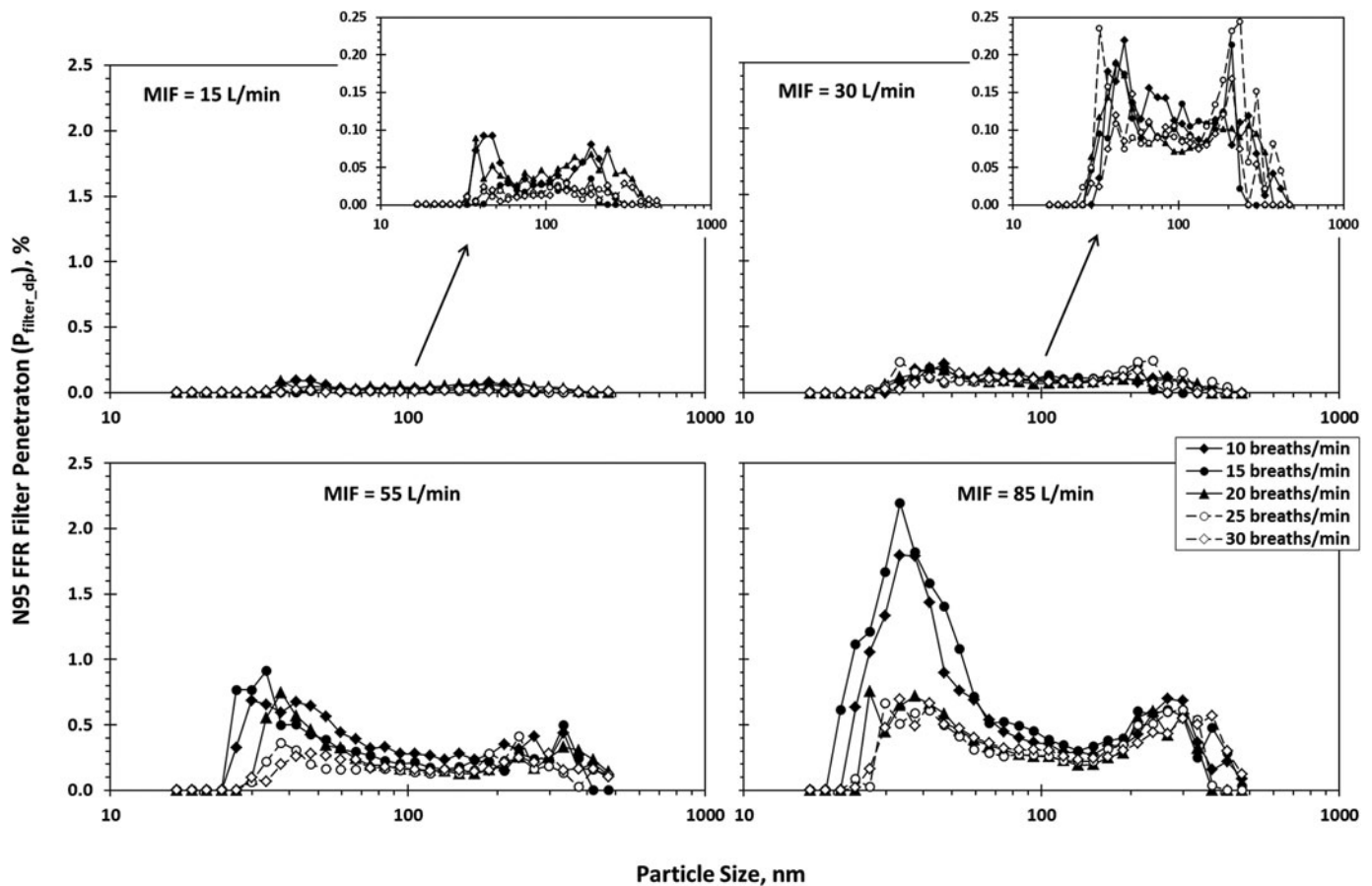
FIG. 1.   Size-specific filter penetration for an N95 FFR sealed to a plastic manikin's face while challenged with charge-equilibrated NaCl particles. Each point represents the mean value of three replicates. Calculated coefficient of variation (CV) has a mean of 0.42 and a standard deviation of 0.31.

higher penetration values for MIF = 15, 55, and 85, but not for 30 L/min. It is hard to differentiate the breathing frequency effect on the penetration at the second MPPS at 200–300 nm for all four MIFs. Such complexity of breathing frequency effect was also reported in our recent investigation that utilized an elastomeric half-mask respirator equipped with P100 filters (He et al. 2013a). As expected, the N95 FFR had P_{filter} below 5% for any particle size, breathing frequency, and MIF tested in the present study.

N95 FFR Total Inward Leakage (TIL$_{dp}$)

The size-specific TIL results for the tested N95 FFR donned on an advanced manikin headform are presented in Figure 2. The TIL$_{dp}$ increased as the particle size increased from 20 to ∼50 nm regardless of the MIF and the breathing frequency, which is consistent with the fact that the diffusional deposition effect is stronger for smaller particles. However, at the particle size of ∼50 nm, the TIL$_{dp}$ curves reached a plateau. The effect of particle size on the TIL$_{dp}$ was not significant ($p > 0.05$) for particles larger than 50 nm for any MIF and breathing frequency used in this study. One possible reason is that the penetration through the faceseal leakage (unlike the filter media) is not

very sensitive to the particle size. Once the particles are large enough (for a typical leakage dimension, the estimated size must be above 40–70 nm) to have a low diffusional deposition efficiency (Kulkarni et al. 2011), their penetration through the faceseal leak is essentially particle-size independent in a wide size range. This differs from P_{filter}, which is influenced by other particle deposition mechanisms. As seen from the data presented in Figures 1 and 2, TIL values are at least ten-fold greater than P_{filter} results. This suggests that the leakage represents the major penetration pathway and thus has the major effect on the TIL, which explains the lack of its particle size dependence at >50 nm. This finding is consistent with the conclusion of our recent study in which the performance of an elastomeric respirator was examined while it was donned on the same advanced manikin headform (He et al. 2013a). Little information is available about the MPPS for faceseal leakage of N95 FFRs. One investigation that measured TIL and filter penetration for N95 FFRs with artificially created leaks, reported MPPS ∼50 nm for leak diameters as small as <1.65 mm (Rengasamy and Eimer 2011). Experimental protocols with artificial faceseal leaks have a number of limitations because (1) the outcome may be dependent not only on the leak size but
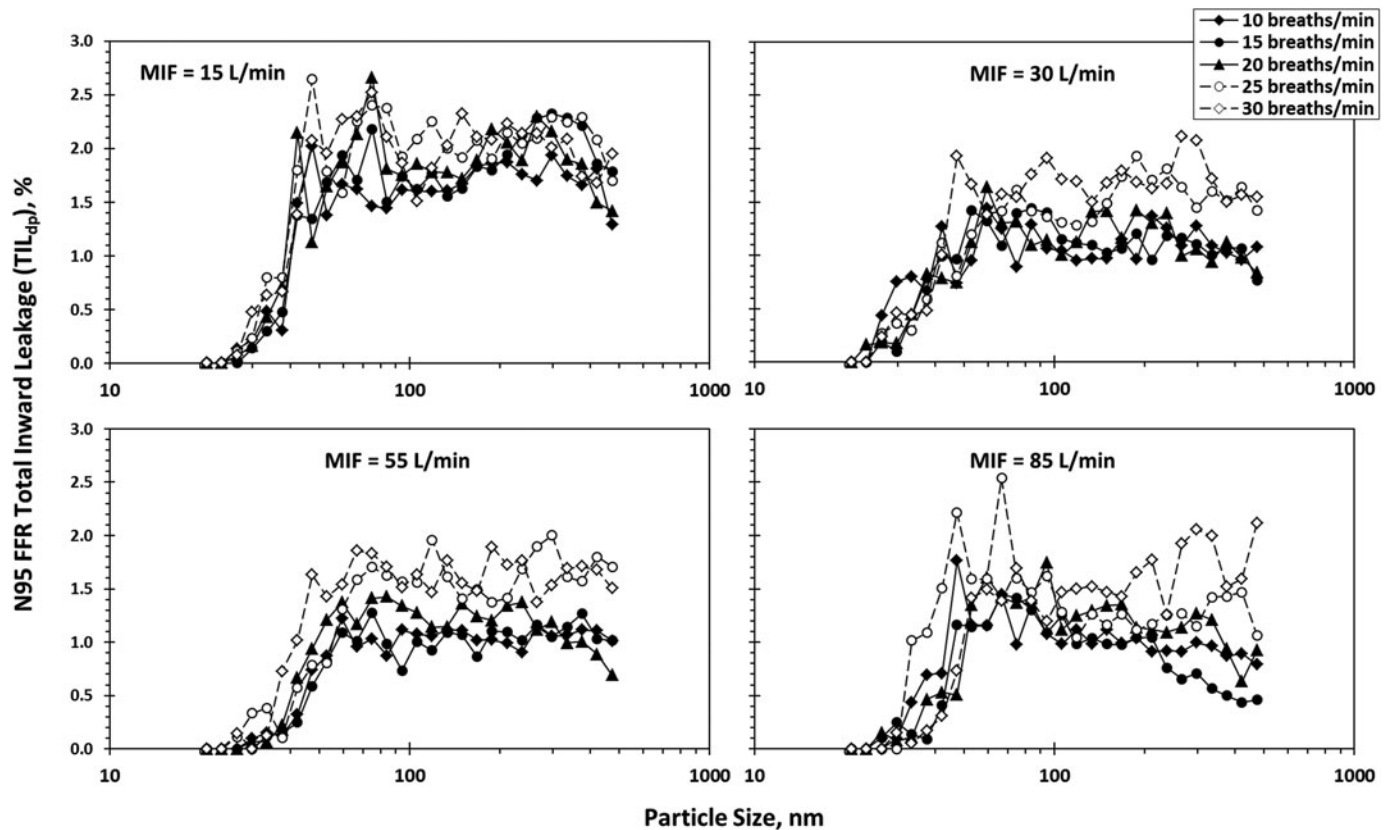
FIG. 2.   Size-specific total inward leakage for an N95 FFR donned on an advanced manikin headform while challenged with charge-equilibrated NaCl particles. Each point represents the mean value of three replicates. Calculated coefficient of variation (CV) has a mean of 0.40 and a standard deviation of 0.32.

factors such as the leak shape, location, and others unaccounted for and (2) in reality, the leak is continuously changing as a wearer is breathing, talking, and moving.

Statistical analysis showed that increasing MIF was associated with a decrease in TIL_{dp} ($p < 0.05$). Other FFR performance studies have reported decreased inward leakage with increasing the breathing flow (Cho et al. 2010b; Rengasamy and Eimer 2011; He et al. 2013c). As communicated earlier, a possible explanation is that higher MIF creates a greater negative pressure during the inspiratory cycle that pulls the facepiece toward the manikin surface with a reduction in leak size (Richardson et al. 2007). This may be particularly evident when testing with the advanced manikin headform with simulated soft skin.

Surgical Mask

SM Filter Penetration (P_{filter_dp})

The filter penetration (P_{filter_dp}) results for the tested SM are presented in Figure 3. Compared to the N95 FFR, the SM had a much higher filter penetration ($p < 0.05$), which is expected given its primary function to protect others from the aerosol exhaled by the wearer. Previous studies have reported that a typical SM provided much lower protection than an N95 FFR when challenged with biological or nonbiological particles (Chen et al.

1990; Willeke et al. 1996; Bałazy et al. 2006a; Lee et al. 2008; Grinshpun et al. 2009; He et al. 2013c). It is also evident from Figure 3 that the filter penetration curves deviate from a single-peak function expected from a conventional mechanical filter. Similar to the interpretation offered for the N95 FFR, we can attribute this difference to cyclic flow tested in this study compared to constant flow utilized by other researchers. As pointed out above, alternatively, the observed phenomenon may derive from an instrumental limitations of Nano-ID associated with corona charging and certain challenges in defining the particle charge as a function of size for particles featuring different characteristics (Dhaniyala et al., 2011). No previous study has reported a multiple P_{filter} peaks for SMs. In the current investigation, three peaks were observed for P_{filter}: at ~30, ~100, and ~300 nm. The most prominent MPPS was ~300 nm for all MIFs and breathing frequencies. This is much higher than the most prominent MPPS obtained for the N95 FFR (30–40 nm). The latter is consistent with the fact that the tested SM had a mechanical filter with no electrically charged fibers (or the charges were negligible). These filters are known for their relatively low-efficiency and MPPS of ~300 nm.

As evident from Figure 3, the curves corresponding to different breathing frequencies were not distinct for MIF = 15 and 30 L/min, and largely also for 55 L/min; the curve separation
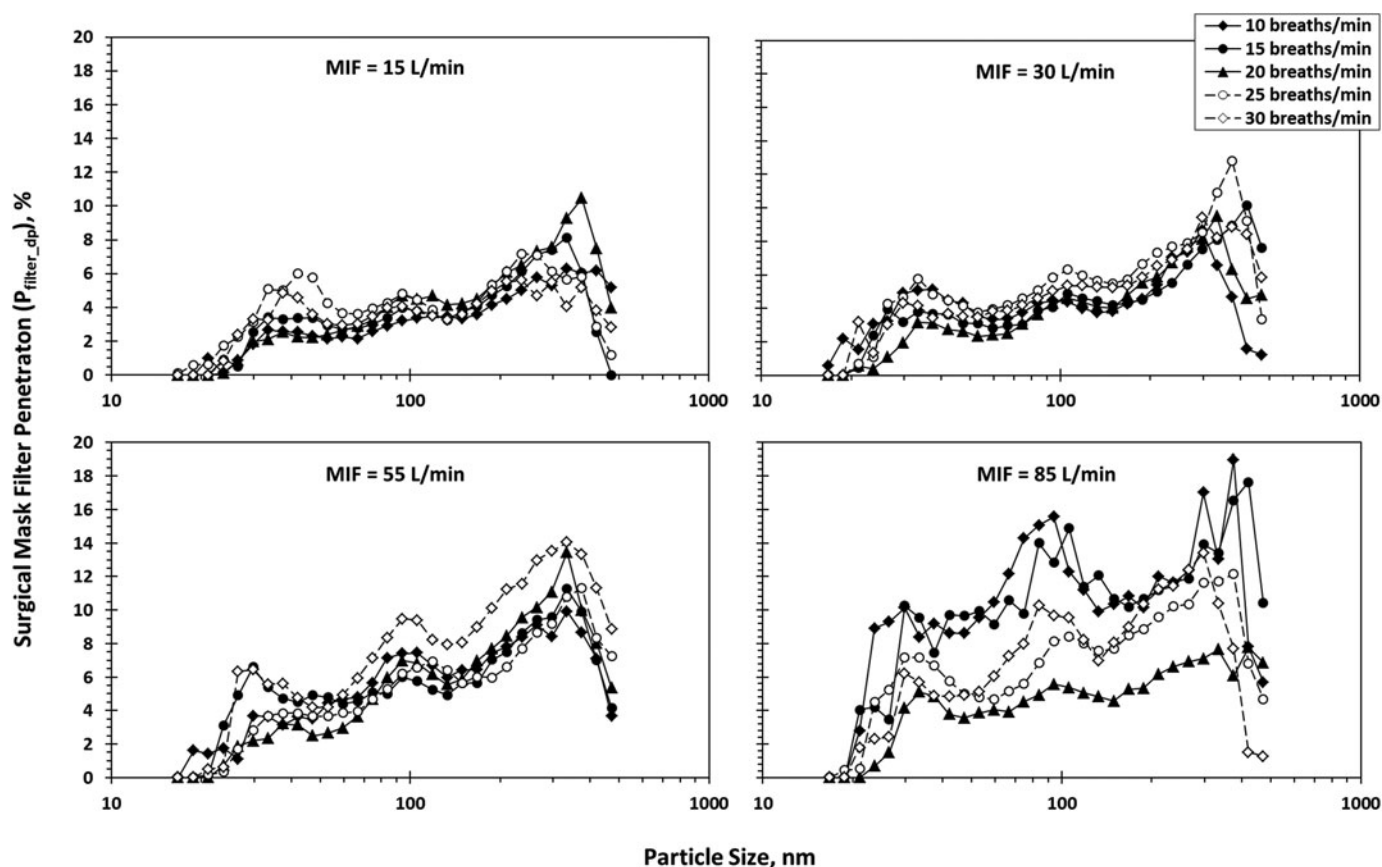
FIG. 3. Size-specific filter penetration for a surgical mask sealed to a plastic manikin's face while challenged with charge-equilibrated NaCl particles. Each point represents the mean value of three replicates. Calculated coefficient of variation (CV) has a mean of 0.45 and a standard deviation of 0.29.

suggests that a more prominent effect of breathing frequency was observed at 85 L/min with the 10 and 15 breaths/min producing higher $P_{\text{filter\_}dp}$ values and 20 breaths/min generating the lowest $P_{\text{filter\_}dp}$ curve. This suggests that the MPPS was not directly affected by the MIF and the breathing frequency.

Although the SM model chosen for this study is expected to provide at least 95% filter efficiency for particles of 100 nm (according to its manufacturer, no flow rate is specified), Figure 3 shows that the filter penetration of 100 nm particles was >5% at various breathing frequencies, especially when MIFs ≥55 L/min. This finding suggests that the tested SM may not provide the expected filter efficiency at higher breathing flows. Particles of 100–400 nm penetrated through the SM filter more readily. From this perspective, the 100-nm size used by the manufacturer as a reference point does not seem appropriate unless the SM is deployed specifically against ≤100-nm particles.

SM Total Inward Leakage (TIL$_{dp}$)

Figure 4 presents the total particle penetration data for the SM. Similar to N95 FFR, the TIL$_{dp}$ of the SM increased rapidly with the particle diameter increasing up to 30–50 nm, but then its dependence on d_p became less pronounced ($p > 0.05$). TIL$_{dp}$ was not significantly affected by breathing frequency

($p > 0.05$) but had slightly different patterns at different MIFs. For particles >30 nm, a slow increase was observed at the lowest MIF (15 L/min), but this gradually leveled off as MIF increased to 85 L/min. This suggests a wide range of sizes producing essentially the same TIL (approximately 20% at MIF = 85 L/min). It is also noticed that the variability in the total penetration obtained for the SM was lower than that for the N95 FFR. The total particle penetration into the SM was about tenfold greater than the penetration into the FFR, which means that the particle count inside the N95 FFR was an order of magnitude lower than that inside the SM (given that C_{out} is the same). Lower count is usually associated with higher variability, which explains our finding. The TIL values (~25%) observed in this study fall into the range reported by other investigators (Oberg and Brosseau 2008; Rengasamy et al. 2009b). To our knowledge, no published study has reported the TIL's MPPS for surgical masks. Even though SMs are not considered personal respiratory protective devices, there are many circumstances where SMs are used to reduce human exposure to hazardous aerosols. In fact, the use of SMs as personal protective devices world-wide likely exceeds the use of N95 FFRs. Given that the size of most "naked" infectious airborne virions (Collier et al. 1998), diesel particles (Castranova et al. 2001), combustion
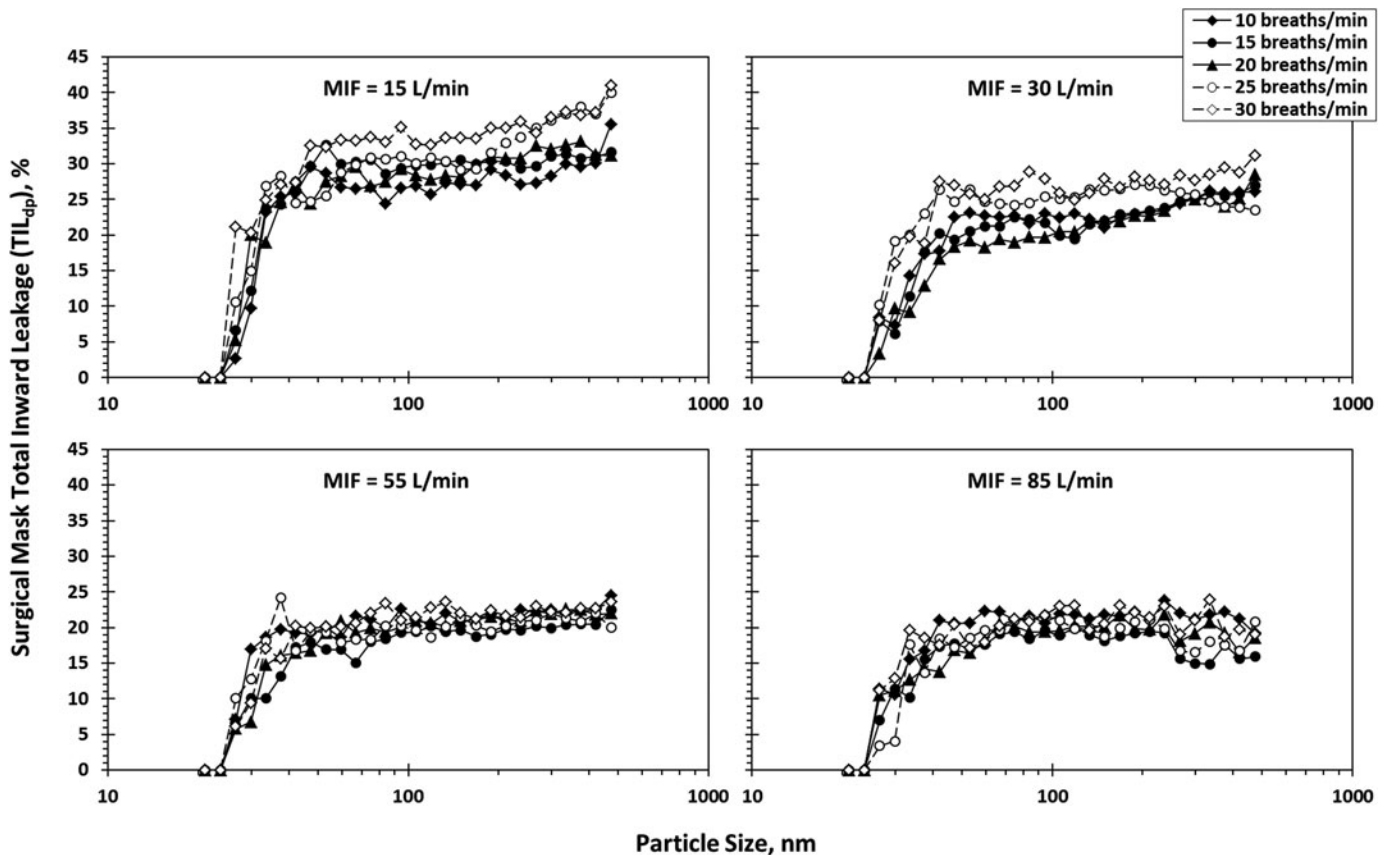
FIG. 4. Size-specific total inward leakage for a surgical mask donned on an advanced manikin headform while challenged with charge-equilibrated NaCl particles. Each point represents the mean value of three replicates. Calculated coefficient of variation (CV) has a mean of 0.18 and a standard deviation of 0.17.

particles generated from fire smoke (He et al. 2013b), and other hazardous aerosols falls into the above-indicated range (20–500 nm), the data suggest that the tested SM may not be able to provide substantial protection against these particles at any relevant combination of the breathing frequency and flow rate.

CONCLUSIONS

For the tested N95 FFR and SM, the filter penetration was significantly affected by the particle size and breathing flow rate, whereas the breathing frequency effect on P_{filter} was generally less pronounced and less important from the practical viewpoint, especially for lower MIFs. Surprisingly, the P_{filter} curves had two peaks for the tested N95 FFR and three peaks for the SM, which has not been reported in previous respirator filter studies. Consequently, using data from a single MPPS may not always be representative of the filter performance, especially if the tested respirator is intended to be deployed against particles of a wide size range.

For the FFR and SM, the total penetration increased with increasing particle size up to ~50 nm; when challenged with particles greater than 50 nm, only the breathing flow rate remained a significant factor affecting the TIL, whereas the influence of particle size and breathing frequency was not significant. In-

creasing the MIF increased the filter penetration, but decreased the total penetration for both the FFR and SM. The SM produced much higher P_{filter} and TIL values than the N95 FFR, and the predominant MPPS was also higher for the SM (~300 nm) than for the N95 FFR (30–40 nm). The results suggest that the tested SM may not be able to provide substantial protection against aerosol particles at least up to ~500 nm at any relevant combination of the breathing frequency and flow rate.

REFERENCES

ASTM. (1989). Standard Test Method for Determining the Initial Efficiency of a Flatsheet Filter Medium in an Airflow Using Latex Spheres. *ASTM Standards (F 1215-89)*.

ASTM. (2001). Standard Test Method for Evaluating the Bacterial Filtration Efficiency (BFE) of Medical Face Mask Materials, Using a Biological Aerosol of Staphylococcus Aereus. *Annual Book of ASTM Standards (F2101-01)*:1553–1557.

Bałazy, A., Toivola, M., Adhikari, A., Sivasubramani, S. K., Reponen, T., and Grinshpun, S. A. (2006a). Do N95 Respirators Provide 95% Protection Level Against Airborne Viruses, and How Adequate Are Surgical Masks? *Am. J. Infect. Control.*, 34:51–57.

Bałazy, A., Toivola, M., Reponen, T., Podgorski, A., Zimmer, A., and Grinshpun, S. A. (2006b). Manikin-Based Performance Evaluation of N95 Filtering-Facepiece Respirators Challenged with Nanoparticles. *Ann. Occup. Hyg.*, 50:259–269.

Bergman, M. S., Zhuang, Z., Wander, J., Hanson, D., Heimbuch, B. K., Mc-Donald, M., et al. (2013). Development of an Advanced Respirator Fit Test Headform. *J. Occup. Environ. Hyg.,* doi:10.1080/15459624.2013.816434.

Castranova, V., Ma, J., Yang, H.-M., Antonini, J. M., Butterworth, L., Barger, M. W., et al. (2001). Effect of Exposure to Diesel Exhaust Particles on the Susceptibility of the Lung to Infection. *Environ. Health Perspect.*, 109:609.

Chen, C. C., Ruuskanen, J., Pilacinski, W., and Willeke, K. (1990). Filter and Leak Penetration Characteristics of a Dust and Mist Filtering Facepiece. *Am. Ind. Hyg. Assoc. J.*, 51:632–639.

Chen, C. C., and Willeke, K. (1992). Characteristics of Face Seal Leakage in Filtering Facepieces. *Am. Ind. Hyg. Assoc. J.*, 53:533–539.

Cho, K. J., Jones, S., Jones, G., McKay, R., Grinshpun, S. A., Dwivedi, A., et al. (2010a). Effect of Particle Size on Respiratory Protection Provided by Two Types of N95 Respirators Used in Agricultural Settings. *J. Occup. Environ. Hyg.*, 7:622–627.

Cho, K. J., Reponen, T., McKay, R., Shukla, R., Haruta, H., Sekar, P., et al. (2010b). Large Particle Penetration through N95 Respirator Filters and Facepiece Leaks with Cyclic Flow. *Ann. Occup. Hyg.*, 54:68–77.

Collier, L., Balows, A., and Sussman, M. (1998). *Topley and Wilson's Microbiology and Microbial Infections, Virology*, vol. 1. Hodder Arnold Publishers, London.

Dhaniyala, S., Fierz, M., Keskinen, J. O., and Marjamaki, M. (2011). Instruments based on electrical detection of aerosols. In: *Aerosol Measurement: Principles, Techniques, and Applications*, 3rd edition, Ch. 18, John Wiley & Sons, Hoboken, NJ, USA, 393–416.

Eninger, R. M., Honda, T., Adhikari, A., Heinonen-Tanski, H., Reponen, T., and Grinshpun, S. A. (2008). Filter Performance of N99 and N95 Facepiece Respirators Against Viruses and Ultrafine Particles. *Ann. Occup. Hyg.*, 52:385–396.

Grafe, T., Gogins, M., Barris, M., Schaefer, J., and Canepa, R. (2001). Nanofibers in Filtration Applications in Transportation. Filtration 2001 Conference Proceedings, Chicago, IL, pp. 1–15.

Grinshpun, S. A., Haruta, H., Eninger, R. M., Reponen, T., McKay, R. T., and Lee, S.-A. (2009). Performance of an N95 Filtering Facepiece Particulate Respirator and a Surgical Mask During Human Breathing: Two Pathways for Particle Penetration. *J. Occup. Environ. Hyg.*, 6:593–603.

Hanson, D., Bergs, R., Tadesse, Y., White, V., and Priya, S. (2006). Enhancement of Eap Actuated Facial Expressions by Designed Chamber Geometry in Elastomers. Proceedings of the SPIE's Electroactive Polymer Actuators and Devices Conf., 10th Smart Structures and Materials Symposium, San Diego.

He, X., Grinshpun, S. A., Reponen, T., McKay, R., Bergman, S. M., and Zhuang, Z. (2013a). Effect of Breathing Frequency and Flow Rate on the Total Inward Leakage of an Elastomeric Half-Mask Donned on an Advanced Manikin Headform. *Ann. Occup. Hyg.*, (accepted) doi: 10.1093/annhyg/met014.

He, X., Grinshpun, S. A., Reponen, T., Yermakov, M., McKay, R., Haruta, H., et al. (2013b). Laboratory Evaluation of the Particle Size Effect on the Performance of an Elastomeric Half-Mask Respirator against Ultrafine Combustion Particles. *Ann. Occup. Hyg.*, doi: 10.1093/annhyg/met014.

He, X., Reponen, T., McKay, R., and Grinshpun, S. A. (2013c). How Does Breathing Frequency Affect the Performance of an N95 Filtering Facepiece Respirator and a Surgical Mask against Surrogates of Viral Particles? *(Submitted) J. Occup. Environ. Hyg.*

He, X., Yermakov, M., Reponen, T., McKay, R., James, K., and Grinshpun, S. A. (2013d). Manikin-Based Performance Evaluation of Elastomeric Respirators Against Combustion Particles. *J. Environ. Occup. Hyg.*, 10:203–212.

Hinds, W. C., and Bellin, P. (1987). Performance of Dust Respirators with Facial Seal Leaks: II. Predictive Model. *Am. Ind. Hyg. Assoc. J.*, 48:842–847.

Huang, S.-H., Chen, C.-W., Chang, C.-P., Lai, C.-Y., and Chen, C.-C. (2007). Penetration of 4.5 Nm to Aerosol Particles Through Fibrous Filters. *J. Aerosol Sci.*, 38:719–727.

Kulkarni, P., Baron, P. A., and Willeke, K. (2011). *Aerosol Measurement - Principles, Techniques, and Applications*, 3rd ed. John Wiley & Sons, New Jersey.

Lee, S. A., Grinshpun, S. A., and Reponen, T. (2008). Respiratory Performance Offered by N95 Respirators and Surgical Masks: Human Subject Evaluation with Nacl Aerosol Representing Bacterial and Viral Particle Size Range. *Ann. Occup. Hyg.*, 52:177–185.

Martin, S. B., and Moyer, E. S. (2000). Electrostatic Respirator Filter Media: Filter Efficiency and Most Penetrating Particle Size Effects. *Appl. Occup. Environ. Hyg.*, 15:609–617.

Myers, W. R., Kim, H., and Kadrichu, N. (1991). Effect of Particle Size on Assessment of Faceseal Leakage. *J. Int. Soc. Resp. Prot.*, 6–21.

NIOSH. (1995). National Institute for Occupational Safety and Health. Us Dhhs, Public Health Service. "Respiratory Protective Devices; Final Rules and Notices". *Federal Register* 60(110):30335–30393.

Oberg, T., and Brosseau, L. M. (2008). Surgical Mask Filter and Fit Performance. *Am. J. Infect. Control.*, 36:276–282.

Rengasamy, S. and Eimer, B. C. (2011). Total Inward Leakage of Nanoparticles through Filtering Facepiece Respirators. *Ann. Occup. Hyg.*, 55:253–263.

Rengasamy, S., Eimer, B. C., and Shaffer, R. E. (2009a). Comparison of Nanoparticle Filtration Performance of NIOSH-Approved and CE-Marked Particulate Filtering Facepiece Respirators. *Ann. Occup. Hyg.*, 53:117–128.

Rengasamy, S., King, W. P., Eimer, B. C., and Shaffer, R. E. (2008). Filtration Performance of Niosh-Approved N95 and P100 Filtering Facepiece Respirators Against 4 to 30 Nanometer-Size Nanoparticles. *J. Occup. Environ. Hyg.*, 5:556–564.

Rengasamy, S., Miller, A., Eimer, B. C., and Shaffer, R. E. (2009b). Filtration Performance of Fda-Cleared Surgical Masks. *J. Int. Soc. Resp. Prot.*, 26:54.

Richardson, A., Wang, A., and Hofacre, K. (2007). Development of Skin-Like Material to Accommodate Respirator Sealing with Manikin Head Forms, in Report to U.S. Army Edgewood Chemical Biological Center.

Wander, J., Hanson, D., and Margolin, R. (2012). *Humanlike Articulate Robotic Headform to Replace Human Volunteers in Respirator Fit Testing*. Air Force Research Laboratory Materials and Manufacturing Directorate, Ohio.

Wang, A., Richardson, A. W., and Hofacre, K. C. (2012). The Effect of Flow Pattern on Collection Efficiency of Respirator Filters. *J. Int. Soc. Resp. Prot.*, 29:41.

Willeke, K., Qian, Y., Donnelly, J., Grinshpun, S., and Ulevicius, V. (1996). Penetration of Airborne Microorganisms Through a Surgical Mask and a Dust/Mist Respirator. *Am. Ind. Hyg. Assoc. J.*, 57:348–355.

Zhuang, Z., Coffey, C. C., Myers, W. R., Yang, J., and Campbell, D. L. (1998). Quantitative Fit-Testing of N95 Respirators: Part I-Method Development. *J. Int. Soc. Resp. Prot.* 16:11–24.